J. COMBIN. MATH. COMBIN. COMPUT. 127a (2025) 4577--4592

Journal of Combinatorial Mathematics and Combinatorial Computing
www.combinatorialpress.com/jcmcc

Convolutional neural network-based optimization model for bird flight aerodynamic simulation

Zhan Zhang[1, ✉]
[1] Faculty of Natural, Mathematical and Engineering Sciences, King's College London, London, WC2R 2LS, United Kingdom

ABSTRACT
This study analyzes the aerodynamics of fluttering flight of birds through their body structure characteristics. A convolutional neural network is combined with a bird-like flight aerodynamic model. By analyzing the symmetric and asymmetric motion laws of birds in flight, the three-dimensional model and equations of motion of the wing-fluttering motion are established, the aerodynamic simulation study of bird wing-fluttering flight under Computational Fluid Dynamics(CFD) and train it by convolutional neural network. When the model trained to 12 rounds, the loss values on both the training and validation sets converge to about 3.5%, the training effect is good. The predicted values of the lift-to-drag ratio by the model in this paper are close to the CFD calculated values, and the average relative errors of the validation set test set are 0.483% and 0.486%, respectively. In addition, the model predicts the pressure coefficient of the flow field better, and the prediction error of the vast majority of the positions is less than 1.2%. In conclusion, the convolutional neural network can significantly improve the performance of bird flight aerodynamic simulation model.

Keywords: convolutional neural network, aerodynamics, simulation model, flapping wing flight, CFD simulation

1. Introduction

Aerodynamics is the combination of air dynamics, gas flow, velocity change and mechanics, and the use of mathematical tools, analysis and computer simulation techniques to build a system that can accurately obtain, control and explain the aerodynamic performance of aircraft in the air [1-4]. Historically, scientists have commonly utilized experimental and numerical simulation techniques to evaluate the aerodynamic performance of aircraft, facilitating their design and optimization. However, the experimental approach is prohibitively expensive, and CFD simulations are excessively time-consuming. To efficiently and cost-effectively predict the aerodynamic performance of various aircraft, this has become a predominant research direction. And convolutional neural networks can precisely achieve this [5-7].

✉ Corresponding author.
E-mail address: zz2481290560@163.com (Z. Zhang).
Received 01 March 2024; Revised 25 May 2024; Accepted 10 November 2024; Published Online 15 April 2025.
DOI: 10.61091/jcmcc127a-259

As natural flying creatures, birds are the natural examples of aerodynamic principles [8-11]. Studies by Jorn A. Cheney [12] on the aerodynamics of raptors in flight, particularly how they adjust their wings and tails at different speeds, have provided deep insights for biomimetic applications in aviation engineering. Christina Harvey [13] discussed various morphing techniques for UAV flight control inspired by birds, reviewing literature on bird flight control and stability, and discussing potential impacts on UAV design. Victor et al. [14] developed a multi-physics computational framework that integrates biomechanics and aerodynamics, which has been successfully applied to the simulation of flapping flight in birds. V.B. Baliga [15] explored the relationship between bird wing shapes, locomotion capabilities, flight behavior, and weight, offering valuable insights for biomimetic design in aviation engineering. Victor

The complexity of avian flight models presents significant challenges in developing accurate dynamic models. In recent years, with the advent of advanced artificial intelligence technologies, researchers have increasingly turned to neural network-based approaches for modeling these complex systems [16-19]. Neural network is a kind of model that can learn and adapt to the data, with strong model adaptation and stability, and thus can better adapt and fit complex nonlinear systems [20-22].

The article deeply analyzes the mechanism of bird flight and explores the excellent flight ability of birds from the body structure and aerodynamics during flight. To this end, an aerodynamic simulation prediction model for bird flight based on convolutional neural network is proposed. The model is designed to efficiently and accurately predict and analyze the aerodynamic characteristics of birds in flight. Utilizing Ansys Fluent, a three-dimensional numerical simulation model of a multi-degree-of-freedom flapping-wing vehicle is conducted under a low Reynolds number non-constant flow field, This simulation examines the angular velocity and angular acceleration of the wing flapping, as well as the kinematic characteristics of the tail.

2. Convolutional neural network cooperative aerodynamic simulation modeling research

2.1. Bird Flight Mechanism Studies

This paper primarily focuses on the study of birds, whose excellent flight ability and high flying skills are attributed to the unique body and wing structure, as well as the excellent flight mode. The study of the flight mechanism of birds can provide theoretical reference for the development of aircraft.

2.1.1. Characteristics of the body structure of birds:

1) Skeletal characteristics. Skeleton is an important structure of vertebrates, play a role in supporting the body and protecting internal organs, the bones of birds have more voids, internal inflatable, in the early stages of development to form a sponge-like air sacs or air cavities, the bone wall is hollow, the wall is thin and light, and some of them are healed together to increase the sturdiness, but also significantly reduce the weight of the bones, the total weight of the bones of the birds is generally accounted for the whole body weight of 5% -6%.

Most of the bird's skull heals into one piece, the interosseous suture disappears, and the teeth undergo degeneration to reduce the load on the body. The cervical vertebrae of birds generally range from 8-25, the number of which is related to the species of birds. The joints between the cervical vertebrae are in the shape of a saddle, which allows the cervical vertebrae to move flexibly over a wide range, and the vertebrae of the torso are healed, and the caudal vertebrae degenerate into the caudal vertebrae to support the tail feathers and shorten the length of the body, which is helpful for maintaining balance in flight. The movement of the caudal vertebrae can control the direction of the tail feathers, which then controls the flight attitude.

2) Wing characteristics. The wings of birds are evolved from the forelimbs of vertebrates, and they are the main source of lift and thrust when birds fly. They are mainly composed of feathers, bones and

muscles, but the proportion of bones and muscles is very small. Feathers can be categorized into feathers such as coverts, flight feathers and shoulder feathers, and primary flight feathers, secondary flight feathers and coverts cover most of the surface area of the bird's body. During the fluttering process of a bird's wings, the feathers will open or close according to the change in flight mode. When the wings flutter upward, the gaps between the feathers open up to allow airflow through the feathers, which can reduce the resistance during the upward fluttering process, and when the wings flutter downward, the feathers close to form the airfoils, and the airflow from the upper and lower airfoils flows through the wings, generating a pressure difference, which in turn generates lift and thrust. The tertiary flight feathers connect the root of the wing to the body, allowing airflow to flow smoothly through the wing.

2.1.2. Flight aerodynamic analysis. Analyzing bird flight mechanisms for bionic mechanism design requires an understanding of the aerodynamic theory of flight.

1) Reynolds number (Re). Re reflects the ratio of inertial and viscous forces on a moving object in a flow field, and is the parameter that must be followed for viscous forces to work [23]. It is usually defined as:

$$\mathrm{Re} = \frac{\rho VL}{\mu} \tag{1}$$

where ρ represents the ambient gas density. V represents the incoming flow velocity. μ represents the dynamic viscous coefficient. L here represents the chord length of the flapping wing, and the Reynolds number reflects the state of the fluid.

2) Lift, drag and thrust force. Bernoulli's equation is as:

$$P_1 V_1 = P_2 V_2 \tag{2}$$

In Bernoulli's equation P_1 and P_2 refer to the atmospheric pressure on each side of the airfoil. V_1 and V_2 refer to the air flow velocity on both sides of the airfoil. From Bernoulli's equation, it can be known that the shape of the airfoil cross-section leads to a pressure difference between the upper and lower surfaces of the airfoil. The longer arc length of the upper surface will cause the air flow speed on the upper surface to be faster, and the air flow speed on the lower surface to be smaller than that on the upper surface, which will result in the phenomenon of small pressure on the upper surface and large pressure on the lower surface, which is the generation of the lift under the gliding condition.

3) Angle of Attack. The wing angle of attack is the angle between the wing centerline and the horizontal direction, and this parameter has a great influence on the aerodynamic performance of the wing. This parameter has a great influence on the aerodynamic performance of the wing. The angle of attack can also be called the angle of attack, which is directly related to the lift and drag coefficients. If the angle of attack is too large, stalling will occur.

4) Lift, drag coefficient and lift-to-drag ratio. Lift coefficient and drag coefficient are directly associated with lift and drag. The ratio of lift and drag or lift coefficient and drag coefficient is called lift-drag ratio. Flapping flight is more complex than other flight modes, and parameters such as body attitude, flap elevation angle, and flutter frequency always change during flight.

2.2. Convolutional Neural Networks

In the aerodynamic simulation of bird flight, convolutional neural network can predict and analyze the aerodynamic characteristics of birds in flight efficiently and accurately through deep learning technology, and optimize the simulation model.

2.2.1. Model structure. The structure of the convolutional neural network model is shown in Figure 1. The convolutional neural network model [24] consists of a convolutional layer that performs convolutional operations, a pooling layer for dimensionality reduction of the data, an activation function to increase the nonlinear factors, a fully connected layer for function fitting, and a softmax classifier, among other components. The model uses the convolution operation to extract data features, the convolution operation is immediately followed by a pooling operation, multiple sets of convolution-pooling operations are performed sequentially, the above operations are completed to access the fully connected neural network, and finally the output is based on the classification results.

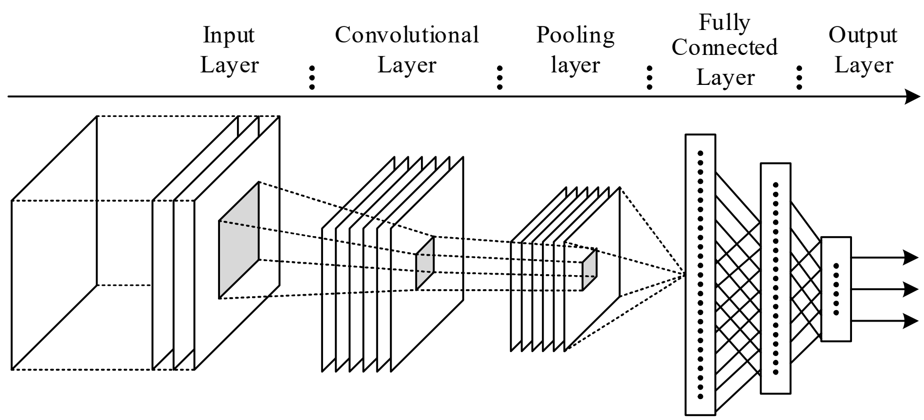

Fig. 1. Convolution neural network model structure diagram

2.2.2. Convolutional layers. The function of the convolutional layer [25] is to perform a convolution operation on the input data to extract the features of the input data. The convolution operation is accomplished by multiplying and summing the convolution kernel with a sub-range of the data point by point. In 2D convolution, for example, the convolution kernel is a two-dimensional matrix, and the number at each position in the matrix corresponds to the weight of each position in the input data. The result of the convolution operation between the convolution kernel and a single block of data is called a feature point. The result obtained from the sliding operation of a single convolution kernel over the localized input data is called the feature map.

2.2.3. Pooling layer. The pooling layer [26] is usually used with the convolutional layer to reduce the dimensionality of the data, effectively reduce the number of parameters in the model, prevent the generation of overfitting phenomenon, and speed up the computation. Maximum pooling is to take the maximum value of the feature points within a specific step data block as the result of the operation. This pooling method can reduce the estimated mean shift caused by the parameter error and retain the data feature information better. The pooling calculation formula is as follows:

$$P(i,j) = f\left(\sum_{m}\sum_{n} I(i+m, j+n)\right) \tag{3}$$

Where $I(i+m, j+n)$ denotes the point input to the local information block in the pooling layer, $P(i,j)$ denotes the result of the local information block after pooling, and $f(\cdot)$ can be taken as the maximum value function, the average value function, and so on. Similar to the process of convolution operation, the pooling operation calculates the local data block from left to right and from top to bottom according to the step size, and obtains the maximum value or average value of the region as the output value of the current data block.

2.2.4. Sigmoid activation function. The role of activation function is to perform a nonlinear transformation at the output of the neural network, lack of activation function is not enough to represent the data.Sigmoid function [27] is the most used activation function. It compresses the output to within $[0,1]$ regardless of the input value and its mathematical expression is shown below:

$$f(x) = \frac{1}{1+e^{-x}} \tag{4}$$

2.2.5. Fully connected layers and softmax. After multiple convolution-pooling operations, the connections are made to the fully connected layer. Any neuron in each layer on the fully connected layer is fully connected to all neurons in the previous layer, while neurons in the same layer are not connected to each other. The local features after convolution and pooling are aggregated and converted into global features. In order to improve the performance of the convolutional neural network model, each neuron in the fully connected layer uses an activation function to increase the nonlinear factor of the whole system and improve the performance of the model.

Finally the output values are classified using softmax classifier [28] which assigns a value in the interval [0,1] to each output classification by calculating the probability of each classification result. The formula is calculated as follows:

$$P\left(Y = k, X = x_i\right) = \frac{e^{s_k}}{\sum_j e^{s_j}} \tag{5}$$

where s_j is the output of the fully connected layer, k denotes the category, and $P\left(Y = k \mid X = x_i\right)$ denotes the probability of sample x_i with respect to category k.

2.3. Aerodynamic modeling of bird-like flight

In this section, the above convolutional neural network is fused with the bird flight simulation model to maximize the play to improve the reliability of the simulation experiment results.

2.3.1. Three-dimensional modeling. Small and medium-sized birds, such as pigeons, are chosen as reference objects for the models in this paper. The typical pigeon parameters and the simplified parameters obtained from actual measurements are shown in Table 1, and the simplified parameters are used for all model dimensions in this paper. The shape of the wings of the imitation bird model is from the literature, and the shape of the body is from the pigeon's flying attitude, all slightly modified. The modeling software SolidWorks is used to establish the imitation bird flapping wing flight model. In the study of bird flight, the influence of the bird's legs on the flow field around the wing flap is ignored in order to simplify the model. The bird-like model includes four parts: the body, the left wing, the right wing and the tail, and all four parts are regarded as rigid body models, the wings on both sides are simplified as thin plates of uniform thickness, and the edges of the wings on both sides of the model use curved edges with rounded transitions, assuming that the wings do not produce flexible deformations during wing-flapping movements.

Table 1. Typical pigeon parameters and simplified parameters

Parameter	Symbol	Typical pigeon	Reduced parameter
String length	c	0.11m	0.10m
Show length	b	0.66m	0.5m
Wing area	S	0.062m2	0.05m/2
Speed	v	11m/s	10m/s
Frequency of motion	f	8Hz	10Hz
Clapping value	φ	0~45°	0~45°
Wing thickness	d		0.004m
Fuselage length	l		0.5m

2.3.2. Symmetric motion. Birds generate the lift and thrust required for flight through the complex and varied motions of their wings, which usually consist of up-and-down flapping, chordal twisting, back-and-forth swinging and spreading folding during flight. In order to simplify the calculation, this paper only considers the up and down flapping and chordwise twisting motions of the wings.

The flapping motion law of bird wings is similar to a kind of trigonometric function of periodic motion, commonly used to describe the flapping motion and torsion motion of the law of motion is shown in the following equation:

$$\varphi(t) = \varphi_{max} \sin(\omega t) + \varphi_0 \tag{6}$$

$$\gamma(t) = \gamma_{max} \sin(\omega t) + \gamma_0 \tag{7}$$

Where: φ_{max} is the maximum angle of flapping motion, °.

γ_{max} is the maximum angle of torsional motion, °.

φ_0 is the initial angle of flapping motion, °.

γ_0 is the initial angle of torsional motion, °.

ω is the flapping angular velocity, rad/s.

Equation (6) and equation (7) are often used to describe the process of symmetric motion of bird flapping flight, when the time spent in the upbeat phase and downbeat phase are equal.

2.3.3. Asymmetric motion. By observing the flight posture of birds and reviewing the relevant literature, considering the existence of a small movement along the vertical direction of a bird's wing driven by its muscles when flapping, define a vertical movement of a wing along the y-axis direction, and define the law of motion of the asymmetric motion as the following equation:

$$\varphi(t) = \begin{cases} \varphi_{\max} \sin\left(\dfrac{\pi}{2kT} t\right) + \varphi_0 & 0 \le t \le kT \\ \varphi_{\max} \sin\left(\dfrac{\pi}{(1-2k)T} \cdot (t - kT) + \dfrac{\pi}{2}\right) + \varphi_0 & kT \le t \le (1-k)T \\ \varphi_{\max} \sin\left(\dfrac{\pi}{2kT} \cdot (t - (1-k)T) + \dfrac{3\pi}{2}\right) + \varphi_0 & (1-k)T \le t \le T \end{cases} \tag{8}$$

$$\gamma(t) = \begin{cases} \gamma_{\max} \sin\left(\dfrac{\pi}{2kT} t\right) + \lambda_0 & 0 \le t \le kT \\ \gamma_{\max} \sin\left(\dfrac{\pi}{(1-2k)T} \cdot (t - kT) + \dfrac{\pi}{2}\right) + \gamma_0 & kT \le t \le (1-k)T \\ \gamma_{\max} \sin\left(\dfrac{\pi}{2kT} \cdot (t - (1-k)T) + \dfrac{3\pi}{2}\right) + \gamma_0 & (1-k)T \le t \le T \end{cases} \tag{9}$$

$$h(t) = \begin{cases} h_{\max} \sin\left(\dfrac{\pi}{2kT} t\right) + h_0 & 0 \le t \le kT \\ h_{\max} \sin\left(\dfrac{\pi}{(1-2k)T} \cdot (t - kT) + \dfrac{\pi}{2}\right) + h_0 & kT \le t \le (1-k)T \\ h_{\max} \sin\left(\dfrac{\pi}{2kT} \cdot (t - (1-k)T) + \dfrac{3\pi}{2}\right) + h_0 & (1-k)T \le t \le T \end{cases} \tag{10}$$

Where: h_{max} is the maximum displacement of vertical motion, m.

h_0 is the initial displacement of vertical motion, m.

In this paper, $\varphi(t)$, $\gamma(t)$ and $h(t)$ are used to represent the upward and downward flapping motion of the wings, the chordal torsion motion and the vertical motion in the vertical direction respectively, which are used to simulate the fluttering flight of the imitation bird model, and h_{max} is chosen to be the thickness of the wing, d , and the wings flutter upward while doing upward movement, and downward flutter while the wings do downward movement. The angle of φ above the plane of xoz is defined as positive, and the angle below the plane of xoz is defined as negative, γ the angle of counterclockwise rotation of the wing is defined as positive, and the angle of clockwise rotation is defined as negative, and h the movement along the positive direction of the axis of y is defined as positive, and the opposite is defined as negative.

2.3.4. Equations of motion for a flapping wing model. In the long-term observation of bird fluttering flight, it is found that both fluttering and twisting around the axis can be approximated as sine and cosine function motions. Combined with the torsional motion establishment is obtained as follows:

$$\begin{cases} \alpha = \alpha_0 \sin\left(2\pi ft + \varphi_a\right) + \alpha_1 \\ \beta = \beta_0 \sin\left(2\pi ft + \varphi_\beta\right) + \beta_1 \end{cases} \tag{11}$$

Where: f is the frequency $\left(Hz\right)$ of the flutter wing flutter, by adjusting the initial value to meet the flutter process of torsion, bending folding changes.

In order to ensure that the flutter wing is synchronized with the flutter wing torsion in the flutter process, the bending and folding phenomenon of the inner and outer wings as well as the motion function of the flutter parameter amplitude ϕ with the same frequency, a sinusoidal function is used for approximate fitting:

$$h(t) = A_0 \sin\left(2\pi ft + h_0\right) + A_1 \tag{12}$$

By setting the frequency and time of movement through the above settings for the bird imitation motion model, it is possible to intuitively observe the operation of the flapping wing simulation motion model, so as to adjust the motion scheme according to the size of the initial value, so that the motion pattern meets the needs of the subsequent simulation of numerical simulation.

2.3.5. Simulation experiment setup. The 3D model of the bird-like flapping wing aircraft is built in SolidWorks software platform and saved into stp format, then imported into Ansys Fluent. The equations of motion are set for each component in the custom field functions, so that the simulation model is simulated and analyzed according to the specified motion model.

On the Ansys Fluent platform, the flight direction of the flapping wing is selected, the steady state wind speed is set in the X-axis and the size is constant Vx, the angle between the center axis and the X-axis direction is the elevation angle of the flying fuselage δ , and the maximum angle of bending and folding of the flapping wing is β . After importing the simulation model, the corresponding position equations and angular equations of motion are inputted through the model position module to realize the flapping wing's “swing-twist-bend-fold” motion.

Determine the computational domain and boundary, the computational domain parameters of the virtual wind tunnel need to meet a number of conditions: the computational domain is set too large, the simulation of experimental accuracy and completion of the efficiency of the computer hardware has high requirements. Therefore, the computational domain is set as X-axis 5 times the direction of the bird body length, the nose 2 times the length of the body. The Y-axis direction is 4 times the height of the fuselage, and the Z-axis direction is 5 times the length of the flap projection.

3. CNN-based simulation optimization model aerodynamic testing

The hardware environment used in this experiment is Inter(R) Core™ i9-14900k CPU; the operating system is windows 10 with 64GB of system memory; and the software configurations are Matlab R2023b, python 3.11, Anaconda, Tensorflow, and keras.

The dataset in this algorithm consists of 2000 sets of 2D airfoil images and lift-resistance ratio data under specified flow conditions, each of which consists of an airfoil grayscale map of 227 × 227 pixel size and the corresponding lift-resistance ratio, of which 70% is used as the training set and 30% as the validation set. The lift-to-drag ratio on the airfoil is derived by the Ansys software at a certain Mach number, Reynolds number, and angle of attack, and in order to reduce the workload of the validation algorithm, the angle of attack of the airfoil is set to 0°, the Reynolds number is set to 400,000, and the Mach number is set to 0.25 for the purpose of this algorithm.

3.1. Simulation model deep learning training effect

In this section, the learning effect of the simulation model under convolutional neural network is evaluated through model training. The Adam optimizer is chosen for the training optimizer, and in order to balance the learning efficiency and learning effect, the exponential decay learning rate is used, where the initial learning rate is the hyperparameters to be optimized, the decay rate is 0.8, and the number of training iterations per round is 100.The initialized weights of the convolutional kernel satisfy the Gaussian distribution with the mean of 0 and the standard deviation of 0.01, and the respective bias is initialized to 0. Under the optimal hyperparameter combinations, model training takes about 10 minutes. The time used is about 10 minutes.

The loss function curves of the training and validation sets during the training process are shown in Fig. 2. As can be seen from the figure, the loss is large at the beginning of the training, and then rapidly decreases to about 0.012, followed by a small increase, and finally gradually converges to about 0.035. The change of loss in the training set and the validation set is basically the same, and the validation set has a small fluctuation after convergence, but the loss value is also around 0.035. From the trend of the loss function, it can be judged that the prediction accuracy of the simulation model based on convolutional neural network is high, and there is no overfitting phenomenon, and the generalization is good.

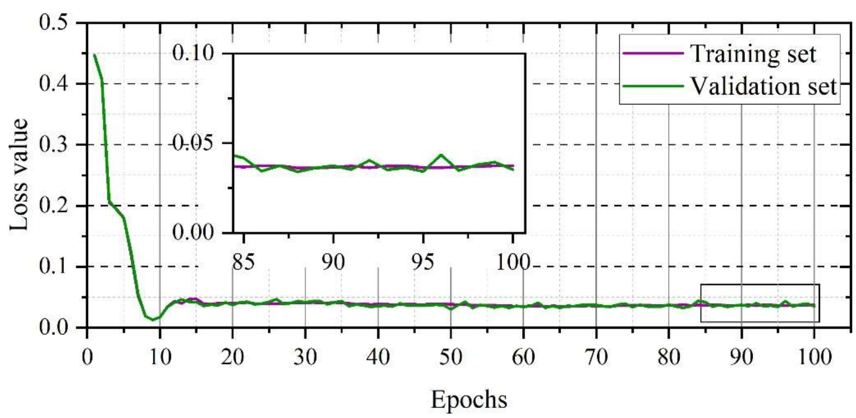

Fig. 2. The loss function of the training set and the validation set

3.2. Airfoil Aerodynamic Predictive Performance Evaluation

3.2.1. Lift ratio coefficient. The network model at the optimal hyperparameter combination with 100 training rounds is selected for performance evaluation. In order to measure the prediction error of the model more intuitively, the relative error (RE) defined in the following equation is used as the metric:

$$RE = \frac{|p-y|}{y} \times 100\% \tag{13}$$

where p is the CNN prediction value and y is the CFD calculation value.

The prediction time for a single sample is less than 1s, and the prediction effect of the lift-resistance ratio for the validation set and the test set is shown in Fig. 3, where the horizontal coordinate is the CFD calculated value and the vertical coordinate is the CNN predicted value, and the closer the scattering point is to the 45° line, i.e., the smaller the error between predicted value and the real value is, the higher the corresponding model's prediction accuracy is, and it can be seen from the figure that, for the validation and the test sets, the predicted value is very close to the real value, and it basically focuses on the 45° line, and all points are located within the ±5% error line. The predicted and true values are very close to each other for both validation and test sets, basically centered on the 45° line, and all points are located within the ±5% error line.

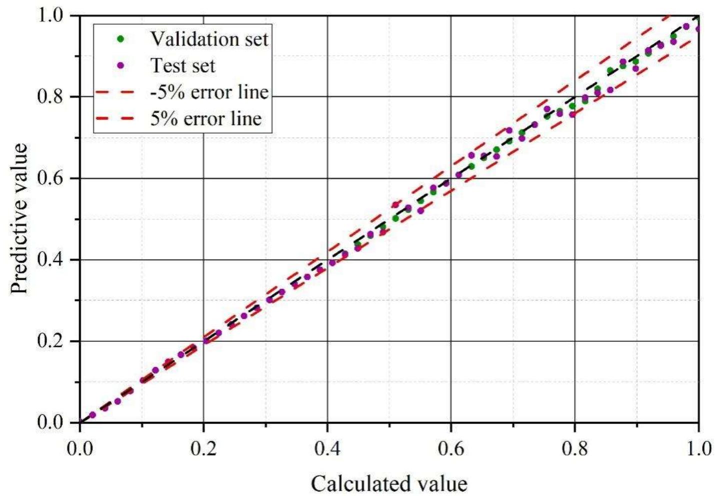

Fig. 3. The resultant drag ratio of the validation set and the test set

The relative errors of the lift-resistance ratio prediction for each sample in the validation and test sets are shown in Fig. 4, and it can be seen that the distribution of the relative errors in the validation and test sets is almost the same, and except for some samples that have larger relative errors in the lift-resistance ratio prediction, the rest of the samples have smaller relative errors, and more than 97% of the samples have a relative error of less than 3%. The average relative errors of the validation and test sets are 0.483% and 0.486%, respectively. In summary, the network model obtained from the training has a high accuracy and is able to achieve fast and accurate prediction of the lift-to-drag ratio of the unknown airfoil type.

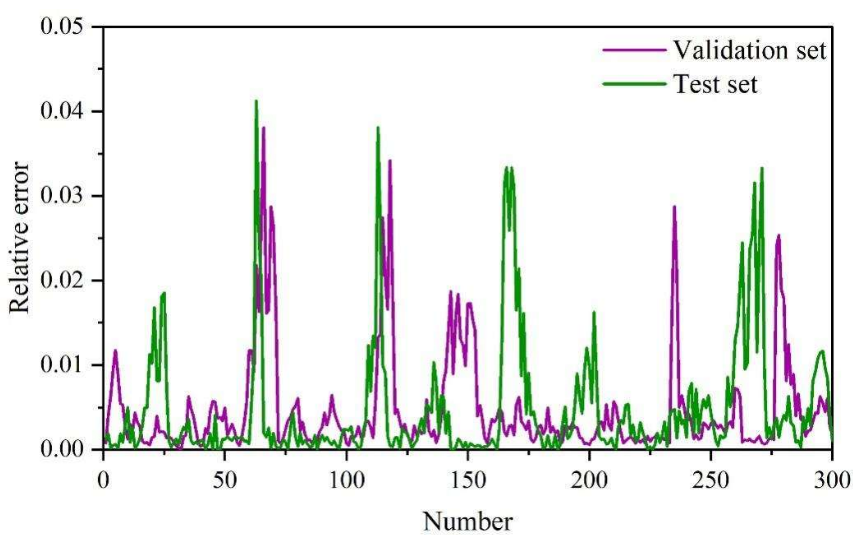

Fig. 4. The vertical drag ratio of all kinds is relative error

3.2.2. Surface pressure coefficient. Calculate the mean and standard deviation of the absolute error at each point on the upper and lower surfaces of the airfoil using the following equations:

$$\mu = \frac{1}{n}\sum_{i=1}^{n}\left|y_p^i - y_t^i\right|$$
$$\sigma = \sqrt{\frac{\sum_{i=1}^{n}\left\|y_p^i - y_t^i\right| - \mu\right|^2}{n-1}} \tag{14}$$

Where n is the number of samples, y_p^i and y_t^i are the CNN predicted and CFD calculated values of the pressure coefficients at the surface points in the ith sample, respectively.

The distribution of the mean and standard deviation of the absolute errors of the pressure coefficients at the points on the upper and lower surfaces of the airfoils in the validation and test sets are shown in Figs. 5 and 6, respectively. It can be seen that the distribution patterns of the mean values and standard deviations in the validation and test sets are basically the same. The overall mean value of the error on the lower surface is small, basically fluctuating around 0.0025. The mean value of the error on the upper surface is larger than that on the lower surface, especially in the 40%~80% chord length interval, the mean value of the error at each point increases significantly due to the influence of the excitation wave, and it reaches the peak point at about 55% chord length position, with the maximum value around 0.02. The distribution of the standard deviation is approximately the same as the distribution of the mean value, and the position with large mean value corresponds to a larger standard deviation. The standard deviation of the lower surface is small about 0.0025, and the upper surface has a larger overall value, especially in the interval of 40%~80% chord length, the standard deviation of the error at each point increases obviously, and the maximal value can be up to 0.017.

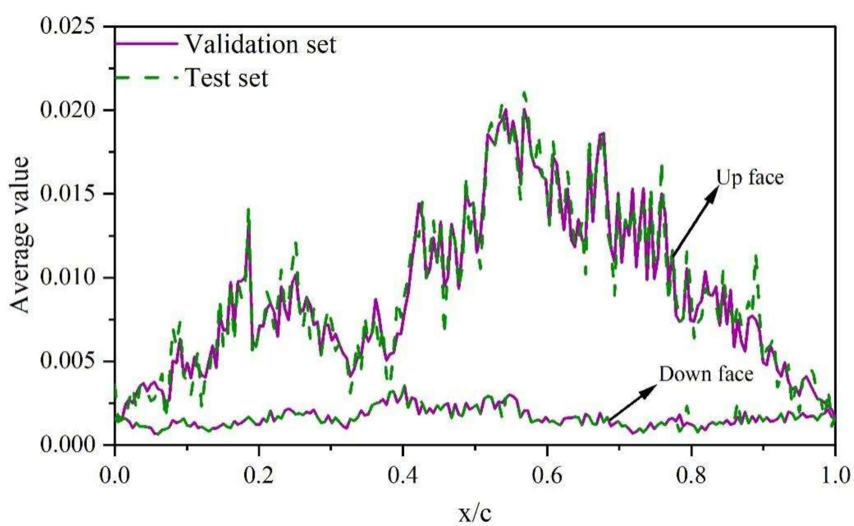

Fig. 5. The absolute error mean of the test set and the test set

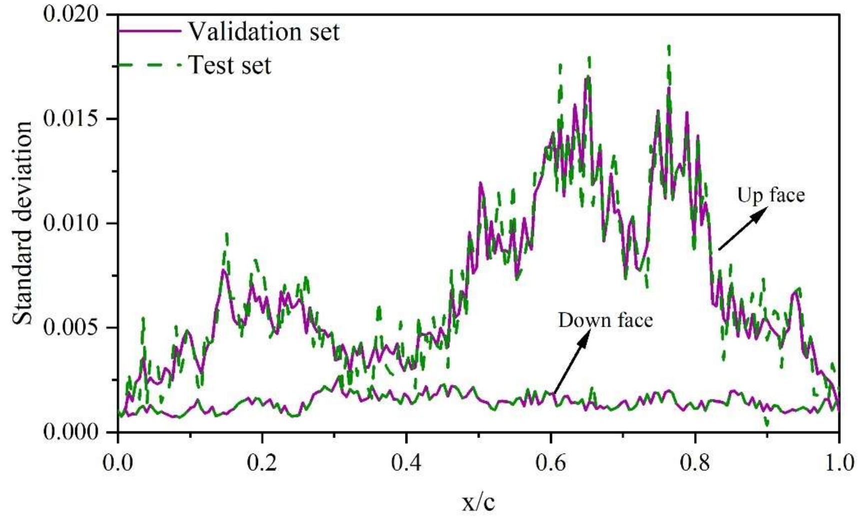

Fig. 6. The validation set and the test set are distributed by the surface deviation

3.2.3. Flow field pressure coefficients. Through the above results, it can be seen more clearly that the convolutional neural network has a better accuracy in the prediction of the wing lift-to-drag ratio, and in the following, the prediction error of the convolutional neural network model will be further analyzed from the aspect of the pressure coefficients of the flow field in comparison with the results of the numerical calculations of the CFD.

Figures 7, 8, and 9 show the CFD calculated values, CNN predicted values, and absolute error (AE) distributions of the flow field pressure coefficient distribution for some samples in the test set, respectively. It can be seen that in the simulation experiments, the absolute error is larger (between 0.047 and 0.148) near the surge position where the pressure on the upper surface of the wing changes drastically, but it is within the acceptable range, and the absolute errors of prediction for the rest of the positions are smaller (less than 0.012), i.e., the convolutional neural network model obtained from the training has a better prediction of the pressure coefficient distribution of the whole flow field, and it is able to realize a more accurate prediction of the surge location and intensity.

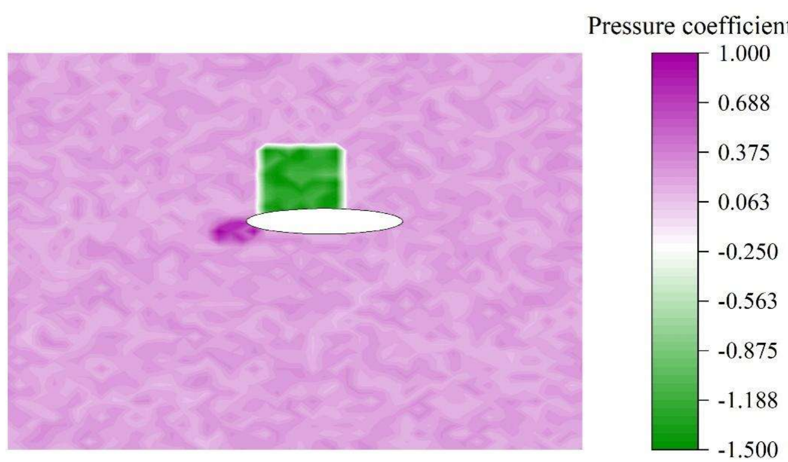

Fig. 7. CFD calculation of the test cluster pressure coefficient

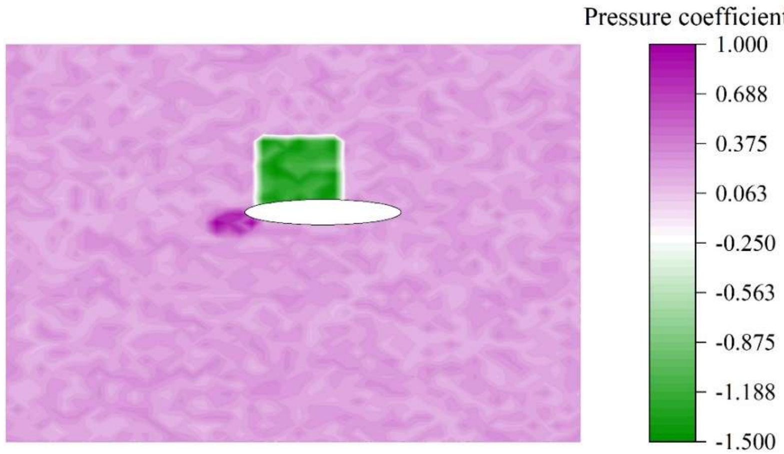

Fig. 8. CNN predictive value test cluster pressure coefficient

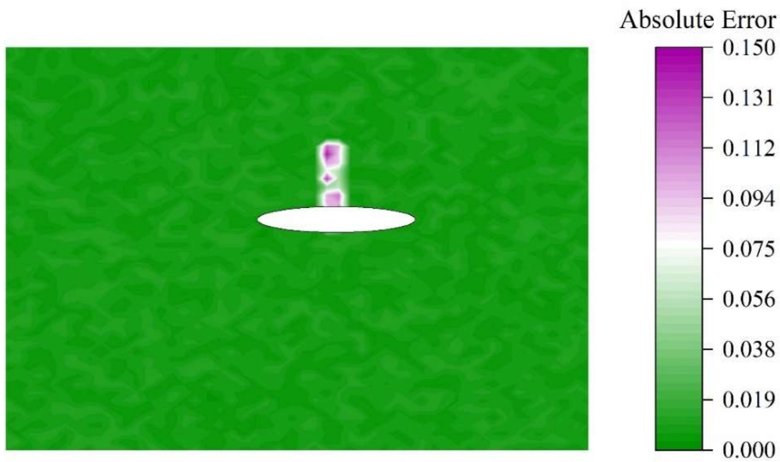

Fig. 9. Test the absolute error distribution of the pressure prediction

3.3. Aerodynamic Simulation Analysis

In order to simulate the motion attitude of bird flight and verify the correctness of the structural design, this paper analyzes the aerodynamic simulation of the whole virtual prototype based on Ansys software, and obtains the motion parameters related to the inner wing, outer wing and tail.

According to the KV value of the brushless motor and the driving voltage, the rotational speed of the motor can be found to be 22000 r/min. The angular velocity curves of the inner wing rod and the angular acceleration curves of the inner wing rod shown in Figs. 10 and 11 can be obtained after simulation calculation. The purple color indicates the simulation change curve of the left inner wing rod, and the green color indicates the simulation change curve of the right inner wing rod. The simulation results show that the flapping angle of the left and right inner wing rods is the same during the flapping process of the prototype wings, and the motion laws of the two sides of the bionic wings are exactly the same, which meets the design requirements.

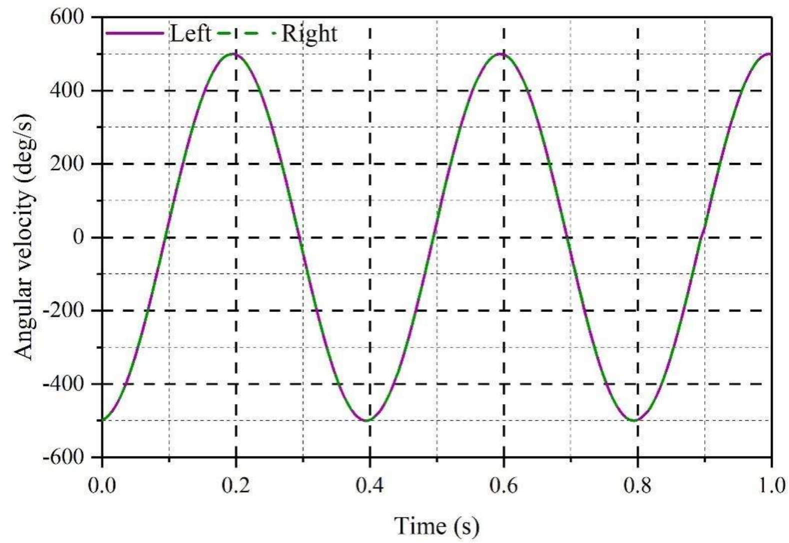

Fig. 10. The Angle of the inner wing bar

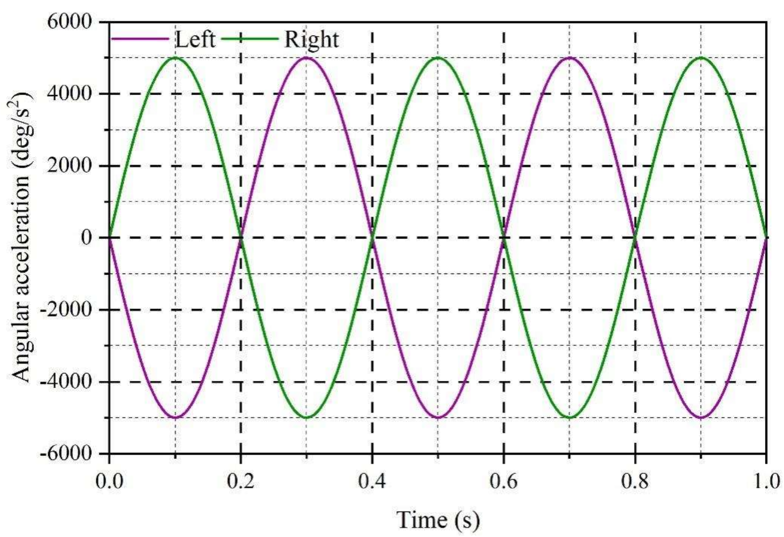

Fig. 11. Angle acceleration curve

The role of the tail is mainly to regulate the steering, by controlling the angle of up and down rotation of the left and right tail can make the flapping prototype produce lift and thrust difference, and then realize the steering action of the flapping prototype. In order to accurately analyze the activity range of the tail, this paper firstly adds the rotation drive MOTION for the two rudder arms in Ansys software, and the function used is the STEP function provided by the software itself, which greatly simplifies the control method of realizing the precise rotation of the rudder arms. When the rotation direction of the two rudder arms is the same, the left tail and the right tail make synchronized up and down movements, thus controlling the pitching motion of the prototype. When the two rudder arms rotate in different directions, the left and right tail fins move up and down alternately to control the yaw motion of the prototype. The final characteristics curve of the tail wing is shown in Fig. 12, which shows that the left and right tail wings oscillate up and down in an angle range of about 60°.

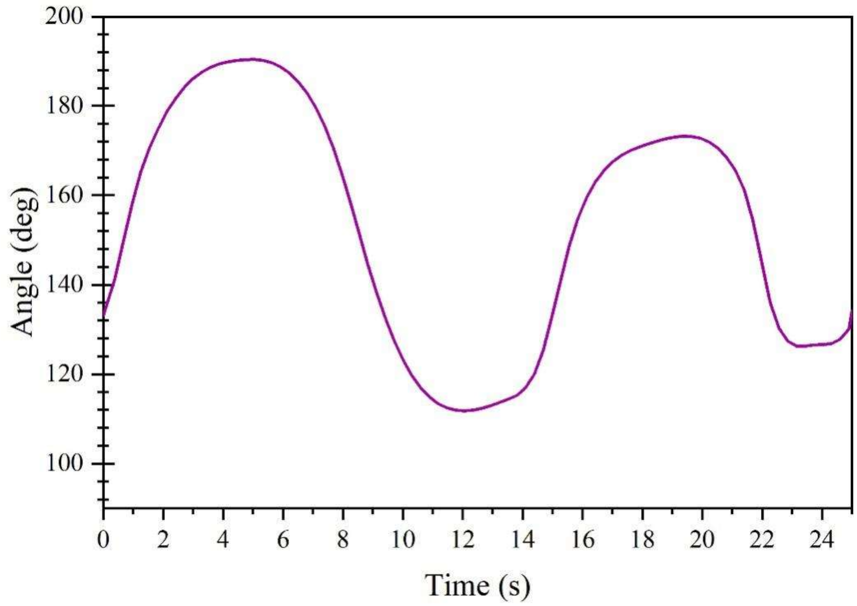

Fig. 12. The motion characteristic of the tail wing

4. Conclusion

The study uses features such as convolutional neural network deep learning and feature extraction to optimize the aerodynamic simulation model of bird flight. By extracting the features of bird wings and body parts, the flight attitude and aerodynamic characteristics of the simulation model are predicted and analyzed more accurately. Combined with several experiments designed in this paper, the aerodynamics of this optimized simulation model is further investigated.

1) Experiment Summary. During the training of this model, the Loss value curve shows a trend of "decreasing-ascending-steady", and converges to 0.035 in 12 rounds of iteration, which shows excellent prediction performance in the aerodynamics of airfoils. Specifically, for the lift-to-drag ratio, more than 97% of the samples are predicted with relative errors below 3%. The maximum relative error for the prediction of surface pressure coefficients is only 0.017. And the absolute error on the flow field pressure coefficients is larger only near the surge position. Through the optimization of convolutional neural network, the kinematic characteristics of wing and the tail of the simulation model meet the design requirements.

2) Shortcomings and Prospects. The performance of convolutional neural network depends greatly on the quality and quantity of training data. In bird flight aerodynamics simulation, it is extremely challenging to obtain high-quality datasets, which are needed to accurately simulate the dynamics of bird wings and complex air flows. In the future, the diversity and quantity of datasets can be increased through data augmentation, such as synthetic data generation and augmented reality techniques, to improve the generalization ability of the model.

References

[1] Bloor, D. (2019). The enigma of the aerofoil: rival theories in aerodynamics, 1909-1930. University of Chicago Press.

[2] Li, D., Liao, W., Rigden, A. J., Liu, X., Wang, D., Malyshev, S., & Shevliakova, E. (2019). Urban heat island: Aerodynamics or imperviousness?. Science Advances, 5(4), eaau4299.

[3] Martins, J. R. (2022). Aerodynamic design optimization: Challenges and perspectives. Computers & Fluids, 239, 105391.

[4] Wu, J. C. (2018). Elements of vorticity aerodynamics. Springer Berlin Heidelberg.

[5] de Oliveira, L. P., Hudebine, D., Guillaume, D., & Verstraete, J. J. (2016). A review of kinetic modeling methodologies for complex processes. Oil & Gas Science and Technology–Revue d'IFP Energies nouvelles, 71(3), 45.

[6] Guo, X., & Wang, J. (2019). A general kinetic model for adsorption: Theoretical analysis and modeling. Journal of Molecular Liquids, 288, 111100.

[7] Skarding, J., Gabrys, B., & Musial, K. (2021). Foundations and modeling of dynamic networks using dynamic graph neural networks: A survey. iEEE Access, 9, 79143-79168.

[8] Tobalske, B. W. (2022). Aerodynamics of avian flight. Current Biology, 32(20), R1105-R1109.

[9] Shahid, F., Zhao, J., & Godefroit, P. (2019). Aerodynamics from cursorial running to aerial gliding for avian flight evolution. Applied Sciences, 9(4), 649.

[10] Biewener, A. A. (2022). Biomechanics of avian flight. Current Biology, 32(20), R1110-R1114.

[11] Jiakun, H. A. N., Zhe, H. U. I., Fangbao, T. I. A. N., & Gang, C. H. E. N. (2021). Review on bio-inspired flight systems and bionic aerodynamics. Chinese Journal of Aeronautics, 34(7), 170-186.

[12] Cheney JA, Stevenson JPJ, Durston NE, et al. Raptor wing morphing with flight speed. J R Soc Interface. 2021;18(180):20210349.

[13] Christina Harvey, Lawren L. Gamble, Christian R. Bolander, Douglas F. Hunsaker, James J. Joo, Daniel J. Inman, A review of avian-inspired morphing for UAV flight control, Progress in Aerospace Sciences, Volume 132, 2022, 100825, ISSN 0376-0421

[14] Victor C ,Renaud R ,Philippe C . Model coupling biomechanics and fluid dynamics for the simulation of controlled flapping flight . Bioinspiration & Biomimetics, 2021, 16 (2): 026023-.

[15] Baliga VB, Szabo I, Altshuler DL. Range of motion in the avian wing is strongly associated with flight behavior and body mass. Sci Adv. 2019 Oct 23;5(10)

[16] Stachiw, T., Crain, A., & Ricciardi, J. (2022). A physics-based neural network for flight dynamics modelling and simulation. Advanced Modeling and Simulation in Engineering Sciences, 9(1), 13.

[17] Michek, N. E., Mehta, P., & Huebsch, W. W. (2024). Flight dynamic uncertainty quantification modeling using physics-informed neural networks. AIAA Journal, 62(11), 4234-4246.

[18] Gu, W., Primatesta, S., & Rizzo, A. (2024). Physics-informed Neural Network for Quadrotor Dynamical Modeling. Robotics and Autonomous Systems, 171, 104569.

[19] Raol, J. R., & Singh, J. (2023). Flight mechanics modeling and analysis. Crc Press.

[20] Mohamed, M., & Dongare, V. (2018). Aircraft neural modeling and parameter estimation using neural partial differentiation. Aircraft Engineering and Aerospace Technology, 90(5), 764-778.

[21] Davis, A., Tompkins, D. W., Fegely, C. E., & Gonzalez, G. (2024). Neural Network Modeling of F/A-18E Flight Dynamics. In AIAA AVIATION FORUM AND ASCEND 2024 (p. 4122).

[22] Norouzi, R., Kosari, A., & Sabour, M. H. (2019). Investigating the generalization capability and performance of neural networks and neuro-fuzzy systems for nonlinear dynamics modeling of impaired aircraft. IEEE Access, 7, 21067-21093.

[23] Nils Paul van Hinsberg & Annika Frede. (2025). Square-section prism with rounded edges in a uniform cross-flow: Effect of incidence angle and Reynolds number on the (un)steady aerodynamics and proneness to galloping. Journal of Wind Engineering & Industrial Aerodynamics105993-105993.

[24] Jesline Jeme V & Albert Jerome S. (2024). Efficient MRI image enhancement by improved denoising

techniques for better skull stripping using attention module-based convolution neural network.Computer Methods in Biomechanics and Biomedical Engineering: Imaging & Visualization(1),

[25] Qi Xu,Zhuoming Xu,Huabin Wang,Yun Chen & Liang Tao. (2025). Online learning discriminative sparse convolution networks for robust UAV object tracking. Knowledge-Based Systems112742-112742.

[26] Ali Sarhadi,Mehdi Ravanshadnia,Armin Monirabbasi & Milad Ghanbari. (2024). Using an improved U-Net++ with a T-Max-Avg-Pooling layer as a rapid approach for concrete crack detection. Frontiers in Built Environment1485774-1485774.

[27] Fatihah Tarmizi. (2025). Case of sigmoid volvolus in a young demographic. Visual Journal of Emergency Medicine102178-102178.

[28] Hong Zhao,Kangping Chen,Zhaobin Chang & Dailin Huang. (2024). Collaborative multi-knowledge distillation under the influence of softmax regression representation. Multimedia Systems(6),331-331.